Supporting Information

Characterization and manipulation of single nanoparticles using a nanopore-based electrokinetic tweezer

Rami Yazbeck, Joseph V. Schoppe, Mohammad A. Alibakhshi,
Kamil L. Ekinci, and Chuanhua Duan*

Department of Mechanical Engineering, Boston University, Boston, MA 02215.

*Address correspondence to duan@bu.edu.

S1. Full ionic trace for 100 nm PS-COOH

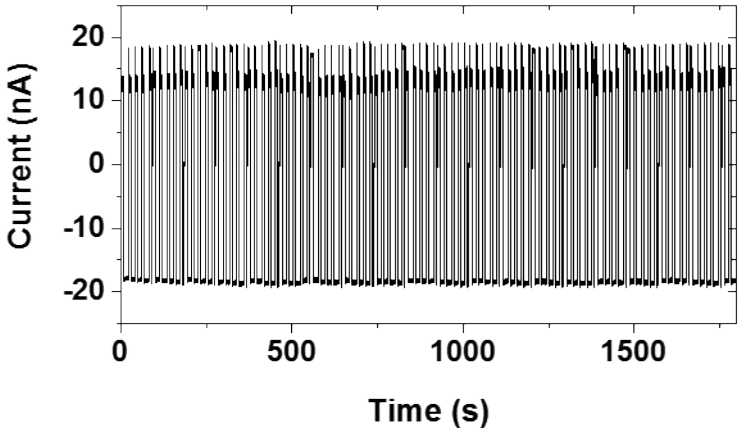

Figure S1: Ionic trace for the trapping experiment of 100 nm PS-COOH particles suspended in 1x PBS, at 200 mV and using a 90 nm silicon nitride nanopore.

Trapping and releasing of a nanoparticle near a nanopore can be repeated as many times as desired. Figure S1 shows the ionic trace of 100 nm PS-COOH particles suspended in 1x PBS using a 90 nm silicon nitride nanopore. The input voltage function consists of a 10s +200 mV pulse which allows the particle to be driven toward the pore and get trapped, and a 10s -200 mV pulse for releasing. Figure S1 plots approximately 100 trapping/releasing cycles.

S2. Single particle trapping-induced blockade event

Nanopore blockade due to electrokinetic trapping of single and multiple nanoparticles has both been previously reported.[1-3] To confirm whether the trapping-induced blockade is a single particle or multiple particles event we have done the following experiments:

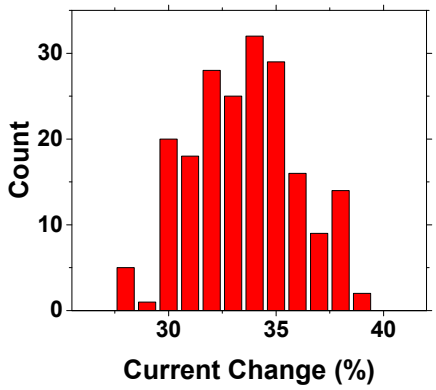

Figure S2: Current change distribution of 200 trapping events of 100 nm PS-COOH particles suspended in 1x PBS, at 200 mV and using a 90 nm silicon nitride nanopore.

First, we have repeated the trapping event up to two hundred times and plotted the histogram of the current blockade levels. We found that the overall standard deviation between the normalized open and trapped current for each event (current change in percentage) is 2.5 nA, which indicates a relatively narrow distribution range (Fig. S2). We are confident that this narrow spread is from the size/ charge distribution of the nanoparticles. So, the fact that the current blockade did not change for a two hundred trapping/releasing cycles indicates that the entrapment is most likely due to the entrapment of a single rather than multiple nanoparticles.

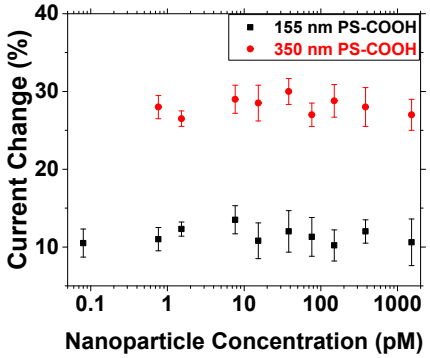

Figure S3: Current change of 155 and 350 nm PS-COOH particles with various concentrations suspended in 1x PBS, tested separately with a 150 nm silicon nitride nanopore at 200 mV.

We have also conducted trapping experiments at different particle concentrations ranging from 80 fM to 1.5 nM using 155 nm PS-COOH particles. Similarly, we have tested particle concentration from 0.8 pM to 1.5 nM using 350 nm PS-COOH particles. Both cases were tested separately using the same 150 nm silicon nitride nanopore. In each of those cases, after the first trapping event, we released the particle using 1 s voltage pulse and then let the system rest for 30 s before applying a voltage pulse to achieve the next trapping event. Fig. S3 displays the current change (in percentage) and the standard deviation for more than 10 trapping events for each concentration, except the lowest concentration (80 fM for the 150 nm PS-COOH) for which only 3 trapping events are analyzed as it takes a long time to achieve trapping state (average 30 min per event). From Fig. S3 it is evident that the current change is not a function of nanoparticle concentration, which further indicates that the entrapment is most likely due to single rather than multiple nanoparticles.

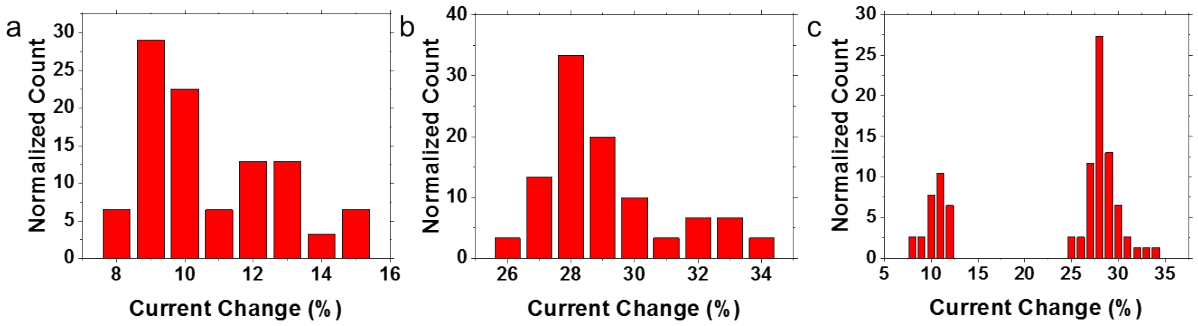

Figure S4: Current change distribution of trapping events using 150 nm pore, 200 mV using **(a)** 155 nm PS-COOH particles, **(b)** 350 nm PS-COOH particles, **(c)** mixed solution of 155 and 350 nm PS-COOH particles; ratio 1:1.

Moreover, we have tested two different sized nanoparticles, 155 and 350 nm PS-COOH, mixed together in the same solution. When tested separately under the same condition both 155 nm and 350 nm PS-COOH produce different and distinguishable current change with a narrow, non-overlapping distribution as shown in Fig. S4a and S4b, respectively. When tested together in a mixed solution with a ratio of 1:1 we were only able to detect two levels of trapping-induced current blockades, each of which corresponded to the blockade level that we measured from the solution with only one of the two nanoparticles (Fig. S4c). These results confirm that the observed trapping phenomenon under our experimental conditions is actually caused by single nanoparticles.

S3. Nanopore blockage using positively charged particles

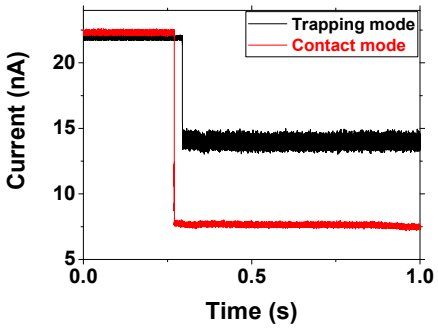

Fig. S5: Current trace signal for single trapping and contact mode event using 155 nm PS-COOH particles and 155 nm PS-COOH particles coated with PEG respectively.

In addition to using negatively charged nanoparticles, we used positively charged nanoparticles for the blockade experiments. In such cases, the nanoparticle would not get trapped near the nanopore, but physically get in contact with the pore due to strong electrostatic interactions with the pore surface. We refer to this blockade state as "contact" blockade mode. To get a positively charged particle we coated our PS-COOH particles with polyethylene glycol modified with amine reagents (PEG-amine). For this experiment we used 155 nm PS-COOH particles and a ratio of 10000 PEG-amine/particle. The modified particles size did not vary and the surface potential changed from -32 mV ± 2 mV to 7 ± 5 mV after conjugation. As shown in Fig. S5, we find that the corresponding current blockades in the contact mode are higher than those in the trapping mode. Also, unlike the trapping mode, the nanoparticle cannot be released by simply using reverse bias. Moreover, in the contact mode the current noise did not increase after particle capture.

Results from this control experiment indicate that the increased noise after a trapping event is unlikely a result of electroosmotic flow induced hydrodynamic vortices. Otherwise we should also observe noise increase after a contact blockade event using positively charged nanoparticles because in both the trapping case and the

contact blockade case, electroosmotic flows from the particle surface and nanopore surfaces are opposite in directions and the resulting flow patterns should have similar effects on the current noise.

S4. Noise analysis

All of the noise analyses were carried out in OriginPro2016. Each power density spectrum in this work was calculated from a one second time signal (in the case of the trapping state signal the first second of trapping). In addition, each signal was smoothed using the "Savitzky-Golay" digital filter in order to further enhance the signal-to-noise ratio without distorting the signal.

Fitting of the theoretical model for an overdamped harmonic oscillator to the experimental data in order to extract the spring constant has been done using the "Levenberg-Marquardt" iteration algorithm. This algorithm is designed to solve nonlinear least square problems by minimizing the sum of the squares of the errors between the experimental data and theoretical function. The coefficient of determination (R^2), which is an indication of how well the theoretical model fits the experimental data, in this study ranges between 0.8-0.9.

S5. Experimental results summary

Table S1: Result summary of the trapping experiments

Setting			**Result**		
Buffer	**Particle**	**Voltage (mV)**	**Current Change (%)**	**Spring Constant (pN/µm)**	**Linear Sensitivity (MΩ/ µm)**
1X PBS	100 nm PS-COOH	200	33.7 ± 2.5	123.2 ± 7.4	70.9 ± 14.5
		300	24.2 ± 1.5	177.4 ± 4.0	55.3 ± 9.6
		400	21.0 ± 2.1	184.1 ± 3.5	40.8 ± 11.2
		500	19.2 ± 1.0	189.3 ± 3.0	32.2 ± 13.5
	155 nm PS-COOH	200	34.7 ± 1.5	42.5 ± 5.2	30.3 ± 8.3
		300	25.2 ± 1.1	66.7 ± 5.0	25.3 ± 5.7
		400	22.0 ± 1.0	88.7 ± 4.1	25.7 ± 7.2
	350 nm PS-COOH	200	37.1 ±1.4	27.2 ± 3.9	20.0 ± 8.9
		300	31.6 ± 1.0	35.8 ± 3.0	19.6 ± 6.8
		400	28.2 ± 0.5	59.1 ± 3.0	21.9 ± 5.1
	100 nm PS-NH2	200	14.2 ± 1.1	110 ± 2.9	70.5 ± 7.2
	100 nm PS-SA	200	12.6 ± 0.5	10.6 ± 0.7	25.7 ± 3.5
3X PBS	100 nm PS-COOH	400	35.6 ± 3.2	187 ± 4.5	31.08 ± 6.1

Table S1 tabulates the trapping results obtained using different experimental settings: buffer concentration, particle type (i.e. size and/or zeta potential), and voltage using 90 nm silicon nitride pore (membrane thickness is 50 nm). The results include the current change between the open and trapped state current, in addition to both the extracted spring constant and the linear sensitivity. The results shown for all cases account for the average of more than 5 different trapping events and the corresponding standard deviation.

S6. Power spectral density plots for the different cases

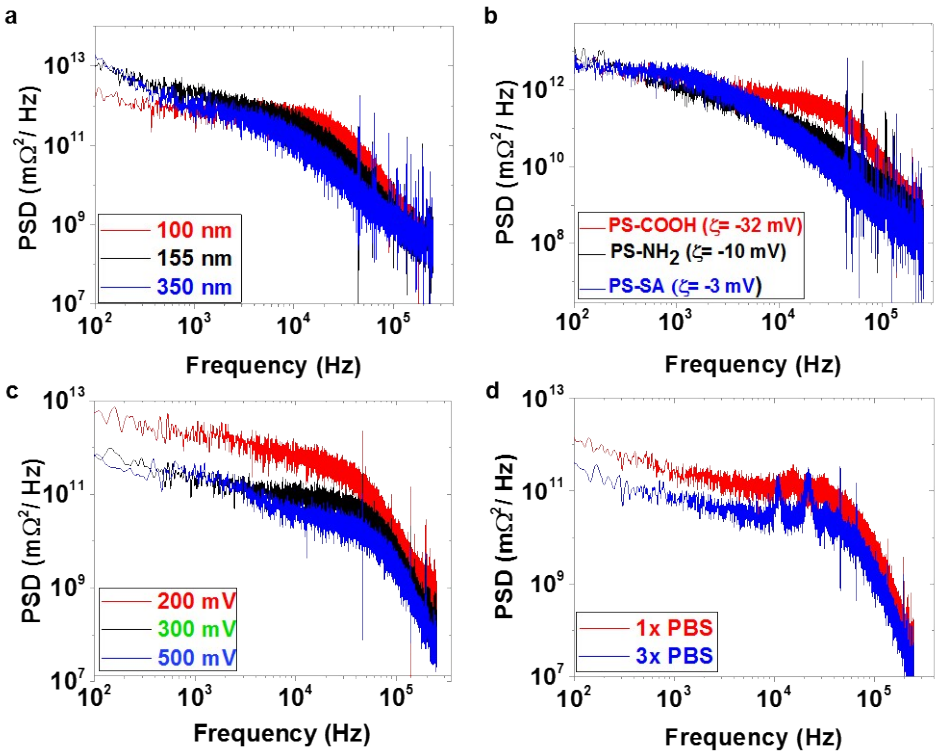

Figure S6: Resistance power spectral density (PSD) plot in the log-scale for the different **(a)** size and **(b)** surface charge density (zeta potential) at 200 mV, using a 90 nm pore. **(c)** PSD plots for trapping signal of 100 nm PS-COOH particles at different **(c)** external voltages and **(d)** buffer concentrations, at 400 mV.

Figure S6a compares the resistance PSDs of the trapping signal for 100, 155 and 350 nm PS-COOH particles at 200 mV. Notice that for the smaller particles, the turning point occurs at a higher frequency, indicating that particles with a smaller size have a higher spring stiffness (i.e. a higher trapping stability). Figure S6b plots the PSDs of the trapping signal for nanoparticles with the same size but different surface charge densities. Particles with a higher surface charge density seem to have a turning point at a higher frequency and thus have a higher trapping stiffness. Figure S6c shows that by changing the voltage we can adjust the trapping stiffness of 100 nm PS-COOH particles. We note that for a higher voltage, the turning point occurs at a higher frequency. Figure S6d compares the PSDs of the trapping signal for 100 nm PS-COOH particles at two different buffer concentrations. The higher salt concentration gives a slightly higher trapping stiffness.

S7. Aspect ratio dependence on trapping-induced normalized current change and trap stiffness

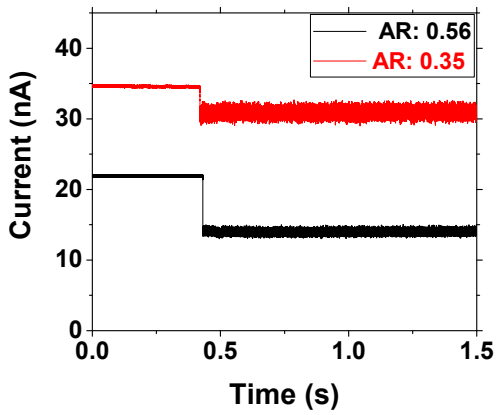

Figure S7: Single trapping event of 155 nm PS-COOH particles at 200 mV, using 0.56 and 0.35 pore aspect ratios.

Table S2: Result summary for two different aspect ratio pores

Aspect Ratio	Current Change (%)	K (pN/µm)
0.56	34.7± 1.5	42.5 ± 5.2
0.35	10.2± 2	32 ± 7.5

Throughout our study we focused on using this trapping phenomenon to detect and distinguish the signal of different nanoparticles, and therefore we have kept the pore aspect ratio (AR) a constant. Pore aspect ratio is defined as the thickness of the membrane (L) divided by the pore diameter (D). To investigate how different pore aspect ratios would affect the trapping signal we have studied the trapping of 155 nm PS-COOH nanoparticles near nanopores with two different diameters (D = 90 and 150 nm, respectively) but the same thickness (t=50 nm), corresponding to aspect ratio of 0. 56 and 0.35 receptively. Fig. S7 shows single trapping event of each of the two ARs tested, and Table S2 summarizes the result obtained from more than 20 different trapping events for each case. For these two studied ARs, we found that a smaller nanopore diameter and thus higher aspect ratio would lead to a higher current blockade, but with a lower spring constant. However, we would not expect that the current blockade will always increase with the increasing aspect ratio as the trapping event will mainly change the access resistance of the system but not the nanopore resistance itself. For higher aspect-ratio nanopores (e.g. L/D > 5 or 10), the pore resistance will be the dominant resistance and we would not expect the trapping event significantly change the current at all. On the other hand, it is actually very challenging for us to create circular nanopores with diameters smaller than 90 nm using our focus ion beam facility. Because of these reasons, we still decide to use nanopores with a diameter of 90 nm for this work, which gave decent current blockades while still having a relatively low aspect ratio.

References

1. M. Tsutsui, Y. Maeda, Y. H. He, S. Hongo, S. Ryuzaki, S. Kawano, T. Kawai and M. Taniguchi, *Applied Physics Letters*, 2013, **103**, 013108.
2. S. Lee, Y. H. Zhang, H. S. White, C. C. Harrell and C. R. Martin, *Anal Chem*, 2004, **76**, 6108-6115.
3. L. Shi, A. Rana and L. Esfandiari, *Scientific reports*, 2018, **8**, 6751.